

## A FORECAST ANALYSIS OF URBAN EXPANSION USING TIME-COMPOSITE CHANGE DETECTION THROUGH MACHINE LEARNING TECHNIQUES

Anam Naz<sup>1</sup>, Rimsha Saleem<sup>2</sup>, Nida Fatima<sup>3</sup>, Hamna Habib<sup>4</sup>, Talia Bilal<sup>5</sup>, Sadia Abdullah<sup>\*6</sup>

<sup>1</sup>University: University of Agriculture, Faisalabad (UAF)

<sup>2</sup>National Textile University Faisalabad

<sup>3,4,5</sup>University of Agriculture, Faisalabad (UAF)

<sup>\*6</sup>Agriculture university Faisalabad

<sup>1</sup>alifanam1228@gmail.com, <sup>2</sup>rimshasaleem029@gmail.com, <sup>3</sup>nidafatimmah28@gmail.com, <sup>4</sup>hamnaakhan1998@gmail.com, <sup>5</sup>taliabilal24@gmail.com, <sup>\*6</sup>sadiaabdullah475@gmail.com

DOI: <https://doi.org/10.5281/zenodo.18385661>

### Keywords

Agriculture, LUCC, Landsat, Supervised Classification, Time-series

Landsat, Machine Learning, Support Vector Machine (SVM), Random Forest (RF), Classification and Regression Tree (CART), Google Earth Engine (GEE).

### Article History

Received: 11 October 2025

Accepted: 21 November 2025

Published: 15 December 2025

Copyright @Author

Corresponding Author: \*

Sadia Abdullah

### Abstract

The concept of Land Use and Cover Change (LUCC) encompassed the modifications occurring on the surface of Earth. Land use pointed to deliberate human actions on land, while land cover described the physical attributes of the land surface. LUCC was a crucial area of research in the context of global environmental change, particularly in developing and underdeveloped countries facing climate changes and urban expansion. Rapid urbanization and the scarcity of agricultural land were major drivers of LUCC on a global scale. This study proposed a novel approach to improve the accuracy of land cover classification and enhance the detection of urban land cover changes. Using remotely sensed Landsat images from 2000 to 2020 and a multi-date composite change detection technique, this research analysed the spatial dynamics and Urban expansion in Faisalabad, Division, Pakistan, over the past two decades. Google Earth Engine (GEE) was utilized to collect data from Landsat satellite. A Normalized Difference Vegetation Index (NDVI) was employed to extract features from the satellite images. Classification and Regression Tree (CART), Random Forest (RF) and Support Vector Machines (SVM) were used as classification algorithms to classify the satellite images into different land cover classes for their ability to monitor expansion across four time periods (2000, 2010, 2015, 2020) in study area. The classification results indicate that SVM outperforms RF and CART, achieving a high accuracy of 98.03%. RF follows with 96.7% accuracy, while CART attains 73.63% accuracy. Based on Landsat results, there had been a decrease in vegetation and agricultural fields, accompanied by an increase in urban areas. The built-up areas had grown to over 60% in 2020, and agricultural land, water bodies, vegetation, and barren ground had experienced continuous reductions. The study highlighted the importance of forecasting agricultural land use changes in Pakistan through historical land use and land cover change detection.

## INTRODUCTION

Land Use and Land Cover Change (LUCC) refers to the transformation of the Earth's surface due to natural processes and human activities. These changes have profound implications for ecosystems, biodiversity, climate, and socio-economic systems. Accurate detection and monitoring of LUCC are essential for sustainable land management, environmental planning, and informed policy-making, particularly in rapidly urbanizing regions of the developing world.

### 1.1 Study Background

LUCC encompasses both deliberate human modifications (land use) and physical alterations of the land surface (land cover). It is a critical area of study within global environmental change, especially in countries facing climate variability and rapid urban growth. Mining, agriculture,

deforestation, and urbanization are major drivers of LUCC, leading to significant environmental, ecological, and socio-economic impacts. Remote sensing provides a powerful, cost-effective alternative to traditional ground surveys for monitoring these changes over large spatial and temporal scales.

### 1.2 Land Use Cover Change (LUCC) Detection

LUCC detection involves identifying transitions between land cover types such as vegetation to urban or agricultural to barren land over time. These changes can result from human activities, climate shifts, or natural disasters. LUCC affects environmental health, economic stability, and social well-being, influencing factors like soil erosion, water availability, biodiversity loss, food security, and human displacement. Accurate detection is therefore vital for mitigation and adaptation strategies.

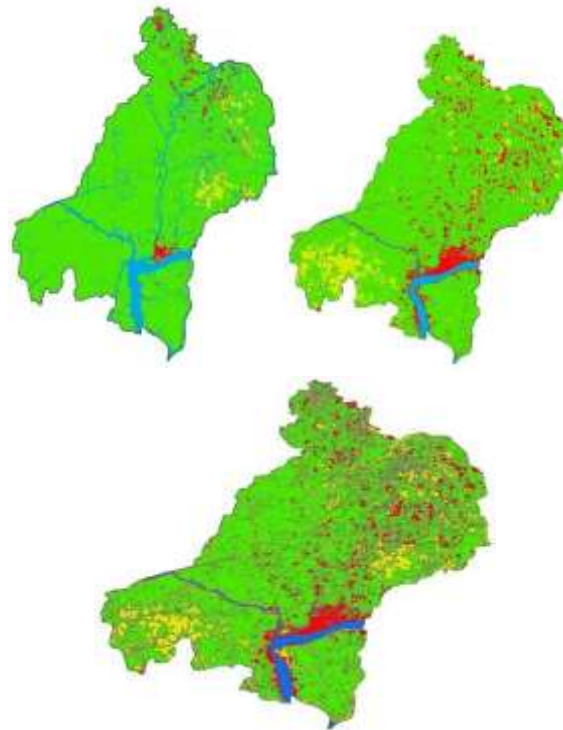


Figure 1.1: Land Image of 1989

Figure 1.2: Land change detection in 2000

Figure 1.3: Land Change Detection from 1989 to 2020

### 1.3 Urban Expansion

Urban expansion the outward growth of cities into surrounding areas—is a dominant form of LUCC

driven by population growth, economic development, and infrastructure improvement. This

process significantly alters landscapes, often at the expense of agricultural land and natural vegetation,

leading to environmental degradation, increased resource demand, and socio-economic shifts.



Figure 1.4: Urban Expansion photograph

**1.3.1 Factors that Drive Urban Expansion:** Key drivers include population growth, economic

development, infrastructure projects (roads, railways), and technological advancements (e.g., automobiles, air conditioning).



Figure 1.5: Factors that drive Urban expansion

**1.3.2 Urban Expansion of Various Types:** Expansion manifests as infilling (development within existing urban areas), edge expansion (growth at city peripheries), linear development (along

transport corridors), sprawl (low-density, extensive growth), and brownfield redevelopment (reuse of previously developed land).

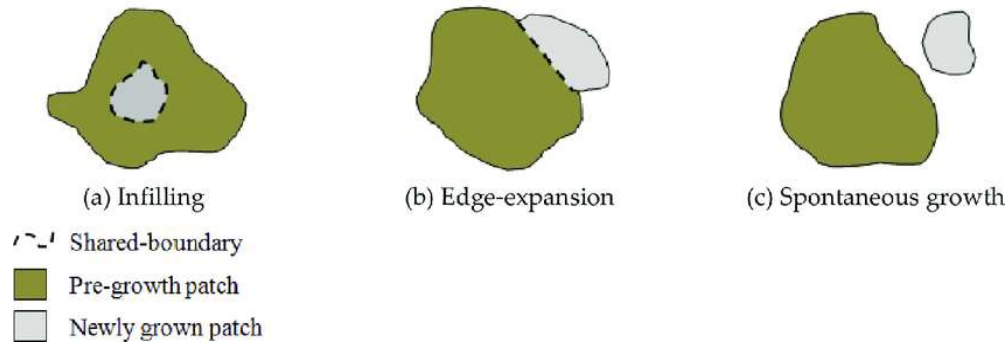


Figure 1.6 Sample of various types of Urban development

1.3.3 Urban Expansion Life Cycle: Urban growth typically follows stages: initiation, growth, maturity, decline, and potential rejuvenation, each with distinct spatial and socio-economic characteristics.

1.4 Artificial Intelligence

Artificial Intelligence (AI), particularly Machine Learning (ML), has become instrumental in analyzing remote sensing data for LUCC detection. ML algorithms can identify complex patterns in satellite imagery, automating and enhancing the accuracy of change detection.

1.4.1 Machine Learning: ML includes supervised learning (trained on labeled data), unsupervised learning (finds patterns without labels), and reinforcement learning. For LUCC, supervised and unsupervised methods are most relevant.



Figure 1.7: Types of Machine Learning

1.4.1.1 Supervised Machine Learning: Algorithms learn from pre-classified examples to map new, unseen data. Common classifiers include Support Vector Machines (SVM) and Decision Trees.

1.4.1.2 Unsupervised Machine Learning: Algorithms group unlabeled data based on inherent patterns, useful for exploratory analysis of land cover.

1.4.1.3 Support Vector Machine (SVM): A robust classifier that finds an optimal hyperplane to separate different classes in high-dimensional space, effective for handling mixed pixels and complex boundaries.

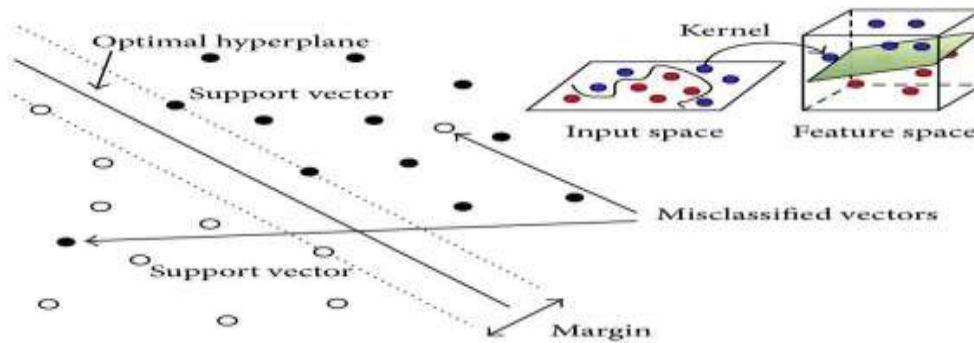


Figure 1.8: The Principle of SVM

**1.4.1.4 Decision Tree:** A model that splits data based on feature values to make predictions; simple and interpretable but prone to overfitting.

**1.4.1.5 Decision Tree Methods:** Includes algorithms like Classification and Regression Trees (CART), which recursively partition data to maximize classification purity.

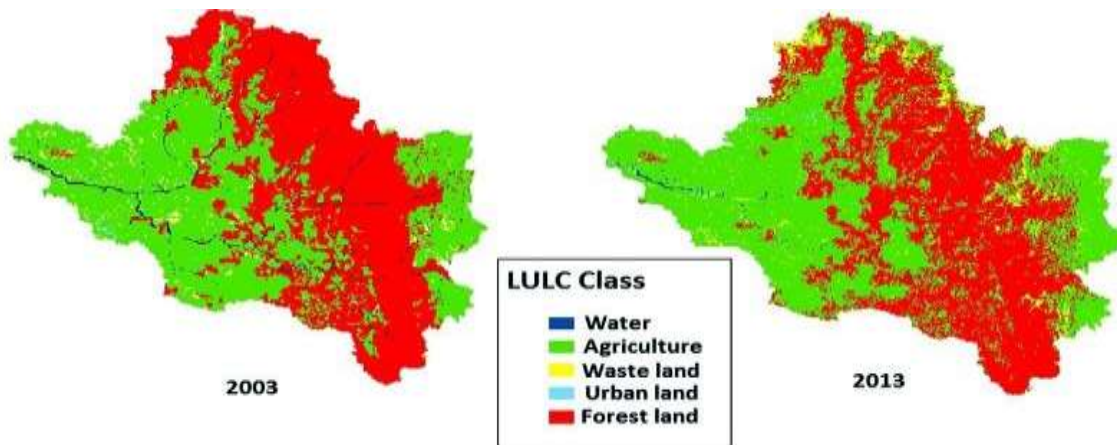


Figure 1.9: LUCC detection of Urban expansion

**1.5 Remote Sensing**

Remote sensing involves acquiring information about the Earth's surface using sensors on satellites

or aircraft, without physical contact. It is fundamental for large-scale, repetitive Earth observation.



Figure 1.6 Sample of various types of Urban development

**1.5.1 Spatial Images:** Digital representations of the Earth's surface capturing spatial patterns of land cover, infrastructure, and resources. They are

essential for analyzing distributions and interactions of geographic features.

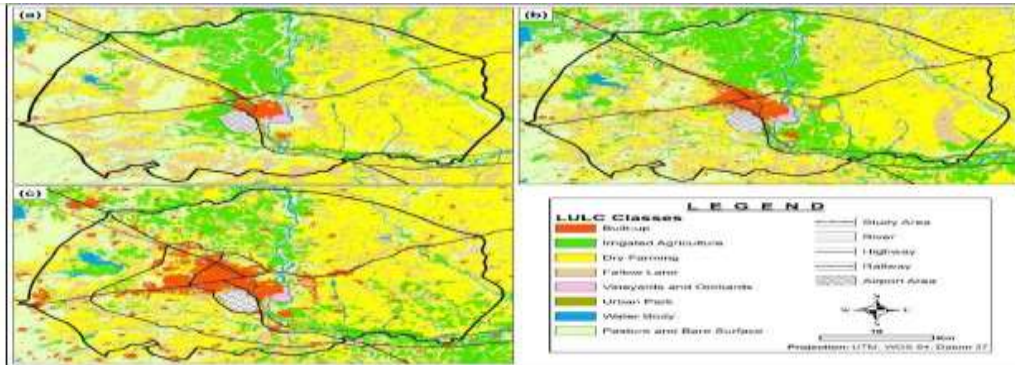


Figure 1.11: The pattern of changes in Land Use and Land Cover (LUCC)

**1.5.2 Aerial Images:**

High-resolution photographs taken from aircraft or drones, providing detailed views for mapping, urban

planning, and environmental monitoring. They can be orthorectified and integrated with multispectral or LiDAR data.



Figure 1.12: Aerial images

**1.6 Need of the Study**

Faisalabad a major agricultural and industrial hub in Pakistan, has undergone significant land transformations over recent decades. However, comprehensive studies analyzing cropland and vegetation dynamics alongside urban expansion are lacking. This gap hinders effective agricultural planning, resource management, and environmental conservation. This study addresses the need for a detailed spatiotemporal analysis of LUCC in Faisalabad to support sustainable development.

**1.7 Gap in Existing Literature**

Challenges persist in applying ML models to new regions due to variations in land cover semantics, spectral confusion between classes, limitations of satellite resolution (e.g., sub-pixel built-up areas), and the need for region-specific validation methods and accuracy assessments.

**1.8 Objectives**

To identify urban LUCC in Faisalabad using multi-temporal Landsat satellite images.  
To analyze the impact of the retrieved dataset on predictive model performance.

To evaluate and compare the accuracy of machine learning classifiers (SVM, RF, CART) for LUCC detection.

## 1.9 Significance

This research provides a framework for monitoring urban expansion and land cover change, offering insights for urban planners, policymakers, and environmental managers. It contributes to sustainable development goals by informing strategies for agricultural preservation, ecological conservation, and resilient urban planning in the face of rapid urbanization.

## Existing Study

A comprehensive review of literature reveals extensive research on Land Use/Cover Change (LUCC) detection, urban expansion analysis, and the application of machine learning and remote sensing techniques. Key studies are synthesized chronologically and thematically below.

## 2.1 Early Methodological Foundations and Decision Tree Applications

Initial research established the utility of remote sensing for urban monitoring. Decision trees were utilized to analyze land use in China's Zhujiang Delta, finding that urban expansion was most rapid in smaller cities near major transportation corridors, rather than in older, larger urban centers [1]. Similarly, a decision tree model was applied to study urban growth in Ajmer, India, identifying population growth, economic development, and land availability as primary drivers [2].

The performance of various classifiers was a focus of comparative studies. Support Vector Machine (SVM), Artificial Neural Networks (ANN), and maximum likelihood classification were compared on Landsat imagery, finding ANN yielded the highest accuracy for land cover classification in Iowa, USA [3].

## 2.2 Advancements in Classification and Change Detection Techniques

Subsequent work focused on improving classification accuracy and change detection methodologies. An ensemble framework integrating spectral, texture, and index data for post-comparison change detection

was introduced, achieving higher accuracy than traditional stacking methods [4]. Another study demonstrated the value of integrating terrain characteristics with satellite imagery to understand the drivers of LUCC, noting the destruction of natural lands due to built-up and farmland expansion [5].

The use of machine learning for predictive modeling emerged. A Random Forest (RF) model trained on topographic and climate data was employed to predict future Landsat spectral values and visualize potential land cover under climate change scenarios [6].

## 2.3 Integration of Cloud Computing and Time-Series Analysis

The advent of cloud computing platforms like Google Earth Engine (GEE) revolutionized large-scale analysis. GEE's significance for LUCC studies over decades was highlighted, demonstrating that fusing pixel- and object-based features improves classification accuracy [7]. The RF algorithm was successfully used on a 26-year Landsat time series in Western Australia to classify mining-induced land clearing, with results aligning with official company records [8].

Time-series analysis was further advanced by the development of a Bidirectional LSTM model for long time-series land cover classification, achieving over 84% accuracy and outperforming CNN and LSTM models [9]. A novel change detection method using radiometric values from aerial images and a T2-WRF classifier was proposed, showing superior performance on benchmark datasets [10].

## 2.4 Contemporary Focus on Advanced Algorithms and High-Resolution Data

Recent literature emphasizes deep learning, high-resolution imagery, and sophisticated change detection frameworks.

**Deep Learning & Advanced ML:** A recurrent convolutional neural network was developed for land cover classification in coastal areas, outperforming RF and SVM in temporal generalizability and detecting changes linked to sea-level rise [11]. It was found that Convolutional Neural Networks (CNN) significantly outperformed SVM and RF for multiannual land cover change detection, achieving

80-90% accuracy [12]. A review of deep learning-based change detection (DLCD) highlighted its advantages over conventional methods but noted challenges like the need for extensive training samples [13].

**Classifier Comparisons:** Multiple studies have compared classifier performance in various contexts. Comparing SVM, RF, and DT on different satellite platforms, SVM was found to have achieved the highest accuracy (~94%) for LULC classification in Malaysia, revealing trends of deforestation and urbanization [14]. SVM was also found to be the most accurate and structured classifier on GEE for LULC mapping in Iran, supporting the use of Dempster-Shafer Theory (DST) for spatial uncertainty analysis [15].

**High-Resolution Data and Specific Applications:** PlanetScope imagery and machine learning (finding KNN outperformed others) were used to classify LULC in heterogeneous urban landscapes in South Africa [16]. A U-Net model was demonstrated to have outperformed Maximum Likelihood Classification (MLC) for LUCC mapping using PlanetScope data, especially when using time-series NDVI [17]. Statistical and machine learning (FR-RF) models were integrated to create a highly accurate landslide susceptibility map [18].

**Urban Expansion Case Studies:** Several studies applied these techniques to specific cities, consistently finding rapid urban growth at the expense of other land covers. Hyderabad, Pakistan, was analyzed from 1979-2020, documenting rapid built-up area increase and decreases in agricultural and vegetated land [19]. Maseru, Lesotho (1988-2019), was studied, finding built-up areas expanded from 15.3% to 48%, primarily due to urbanization [20]. A 560% increase in construction land was documented in Wuhan, China (1987-2016), with

farmland being the primary source [21].

### 2.5 Synthesis and Identified Gaps

The literature confirms that remote sensing and machine learning are powerful tools for LUCC detection. SVM and RF consistently show strong performance, with deep learning methods offering advanced capabilities for complex pattern recognition. Cloud platforms like GEE have enabled large-scale, temporal analysis.

However, gaps remain, including challenges in applying models to new regions due to varying land cover semantics, spectral confusion between classes (e.g., built-up areas with different functions), limitations from coarse spatial resolution, and the need for robust, region-specific validation methods [22]. This study addresses these gaps by applying and comparing multiple ML classifiers (SVM, RF, CART) to the specific context of Faisalabad, Pakistan, using a multi-temporal Landsat dataset on the GEE platform.

## 3: MATERIALS AND METHODS

This chapter details the methodology employed to detect urban land use and land cover change (LUCC) in Faisalabad Division, Pakistan, from 2000 to 2020. A systematic workflow was implemented using remote sensing data and machine learning classifiers within the Google Earth Engine (GEE) cloud platform.

### 3.1 Overview

The research utilized a multi-temporal land cover dataset comprising Ground Truth data and satellite imagery from Landsat 8 and Landsat 5. The methodology was structured into five major components: study area description, data acquisition (GEE and Landsat), pre-processing, development environment setup, and model training.



Figure 3.1: Location of the research Area

### 3.1.1 Study Area

The study focused on Faisalabad Division, a major industrial and agricultural hub in eastern Pakistan. The region is characterized by fertile plains but has experienced rapid urbanization and population expansion. The analysis aimed to quantify LUCC dynamics across four time periods: 2000, 2010, 2015, and 2020.

### 3.1.2 Google Earth Engine

Google Earth Engine (GEE), a cloud-based geospatial platform, was used for data acquisition, processing, and analysis. Its key features include:

**Data Catalog:** Access to a vast archive of satellite imagery, including Landsat

**Code Editor:** A web-based IDE for writing and executing geospatial analysis scripts in JavaScript.

**Processing Power:** Leverages cloud infrastructure for handling large-scale datasets.

**Analytical Tools:** Built-in functions for image classification, spectral index calculation, and time-series analysis.

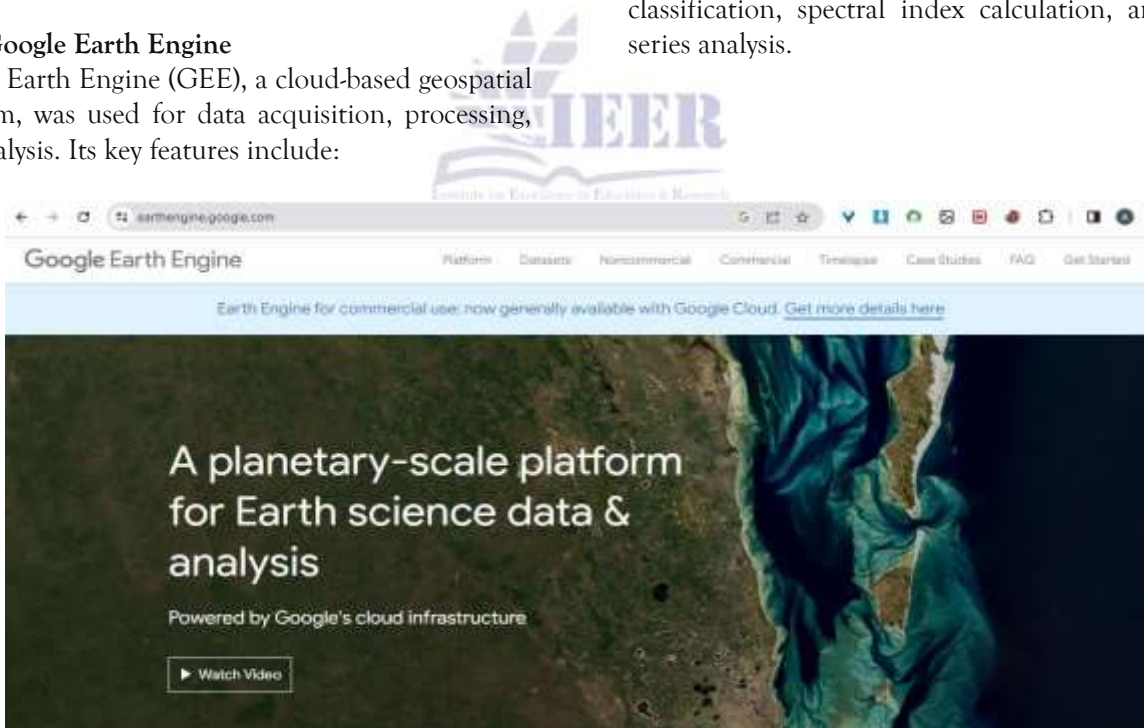


Figure 3.2: Platform of GEE

### 3.1.3 Landsat Data

The study utilized data from the Landsat program, specifically:

**Landsat 8:** Equipped with the Operational Land Imager (OLI) and Thermal Infrared Sensor (TIRS). Provides 11 spectral bands with a 30-meter spatial resolution (15m for panchromatic) and a 16-day

revisit time. Surface reflectance data from Landsat 8

was used for the years 2015 and 2020.

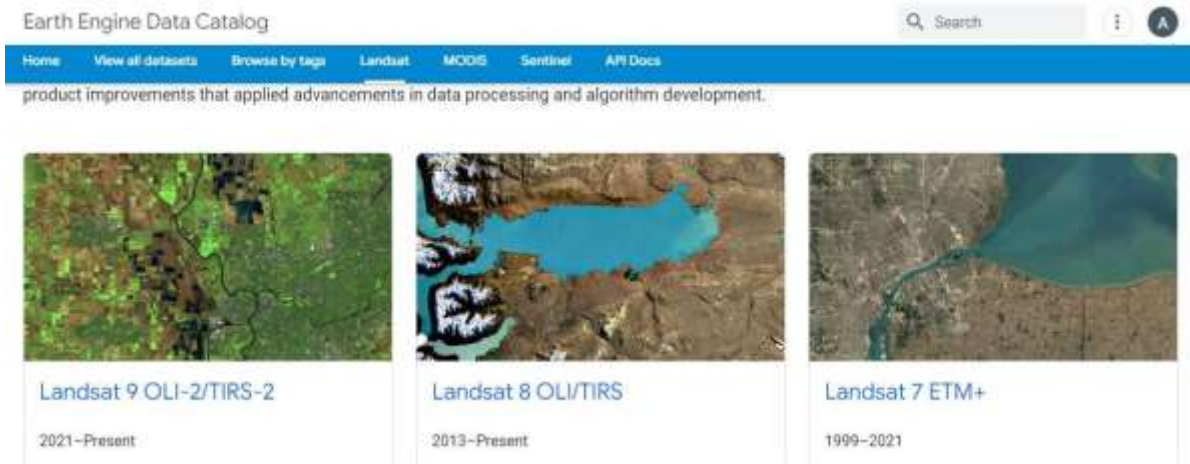


Figure 3.3: Landsat 8 Dataset



Figure 3.4: Landsat 8 Surface Reflectance Dataset



Figure 3.5: Landsat 8 Image collection

Landsat 5: Carried the Thematic Mapper (TM) sensor with seven spectral bands at a 30-meter

resolution. Data from Landsat 5 was used for the years 2000 and 2010.

```

var dataset = ee.ImageCollection('LANDSAT/LT05/C02/T1_L2')
Map.addLayer(geometry)
Map.centerObject(geometry, 18)

// Function to calculate NDVI
var addNdvi = function(NDVI){
  var inf = NDVI.select('SR_B4');
  var red = NDVI.select('SR_B3');
  var ndvi = inf.subtract(red).divide(inf.add(red));
  return NDVI.addBands(ndvi);
}

//choose and filtering image collection for year 2014
var filtered_2000 = dataset.filterBounds(geometry)
  .filterDate('2000-06-01', '2000-06-30')
  .filterMetadata('CLOUD_COVER', 'less_than', 20)
  .select('SR_B*')
  .map(addNdvi)

print(filtered_2000, 'Dataset for 2000')
var before = filtered_2000.median().clip(geometry)
Map.addLayer(before, imageVisParam, 'before')
var filtered_2005 = dataset.filterBounds(geometry)
  .filterDate('2005-06-01', '2005-07-01')
  .filterMetadata('CLOUD_COVER', 'less_than', 20)
  .select('SR_B*')
  .map(addNdvi)
    
```

Figure 3.6: Landsat 5 images for year 2000 and 2010

### 3.1.4 Pre-processing

Key pre-processing steps were applied to prepare the data for machine learning classification:

**Water Body Masking:** The Normalized Difference Water Index (NDWI) was calculated to identify and exclude shoreline pixels of fluctuating water bodies,

ensuring stable training data. Pixels with an NDWI value less than 0.2 were masked out.

**Vegetation Index Calculation:** The Normalized Difference Vegetation Index (NDVI) was computed for all images to assess vegetation density and health, providing a crucial feature for classification. NDVI values range from -1 (water) to +1 (dense vegetation).



Figure 3.7: Landsat 5 dataset

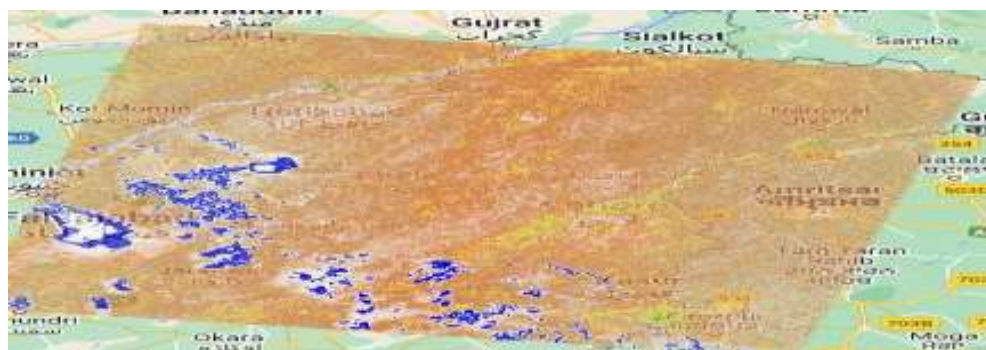


Figure 3.9: NDVI of Landsat 8

```

}

// Function to calculate NDVI
var addNdvi = function( NDVI){
    var inf = NDVI.select('B8');
    var red = NDVI.select('B4');
    var ndvi = inf.subtract(red).divide(inf.add(red));
    return NDVI.addBands(ndvi);
}

// Function to calculate SAVI
var addSAVI = function(image) {
    // Define the SAVI adjustment factor
    var L = 0.5;
    // Get the Red and NIR bands from the image
    var red = image.select('B4'); // Replace 'B4' with the band number for Red
    var nir = image.select('B8'); // Replace 'B8' with the band number for NIR
    var savi = nir.subtract(red).divide(nir.add(red).add(L)).multiply(1.0 + L);
    return image.addBands(savi.rename('SAVI'));
}

```

Figure 3.8: NDVI of Landsat 8 image of 2020

### 3.2 Development Environment and Methodology Flowchart

The core analytical workflow was implemented in GEE and followed a structured pipeline: (a) satellite

data acquisition and pre-processing, (b) training sample collection, (c) classification using machine learning algorithms, (d) model evaluation, and (e) accuracy assessment.

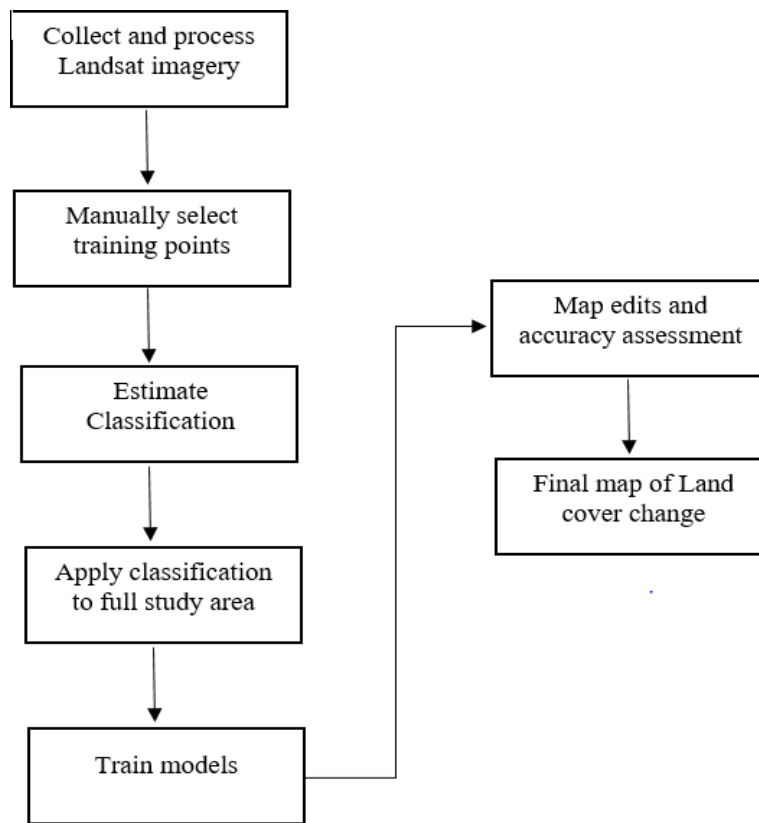


Figure 3.10: Methodology flowchart

### 3.2.1 Dataset

Data collection and preparation were performed entirely within GEE. Landsat imagery for the target years was loaded, and sample points for four land

cover classes (Water, Built-up Area, Barren Land, and Vegetation) were manually labeled using the GEE code editor to create training data.



Figure 3.11: open code editor to load the image

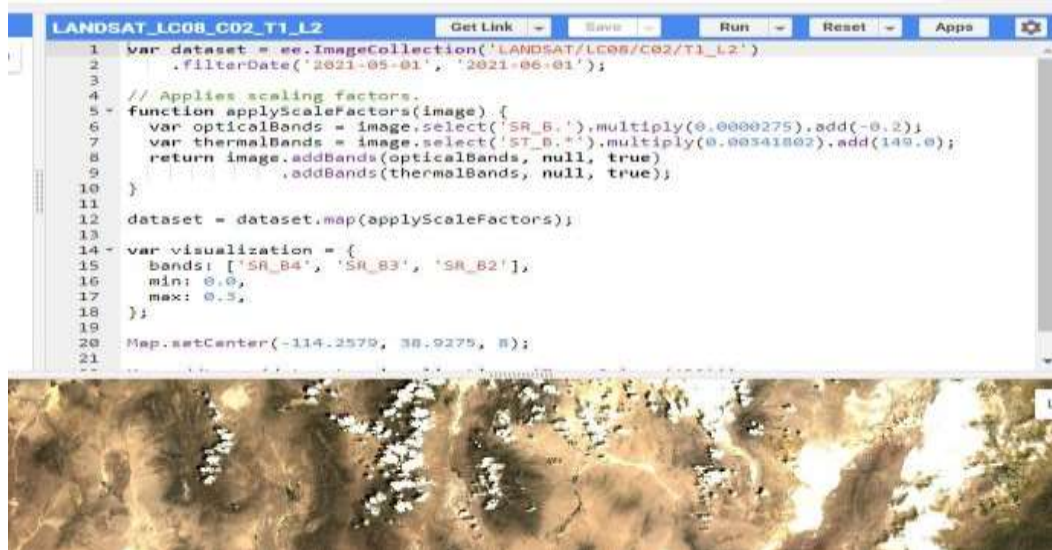


Figure 3.12: Loading dataset from GEE

Date	Satellite	Sensor	Cloud cover present
2000-04-01	Landsat 5	TM - SR	1
2010-04-01	Landsat 5	TM - SR	1
2015-04-01	Landsat 8	OLI/TIRS - SR	5
2020-04-01	Landsat 8	OLI/TIRS - SR	5

Table 3.1: Integration of satellite Images bands to collect sample points for every year

### 3.3 Model Training

Three supervised machine learning classifiers were trained and applied for land cover classification and change detection.

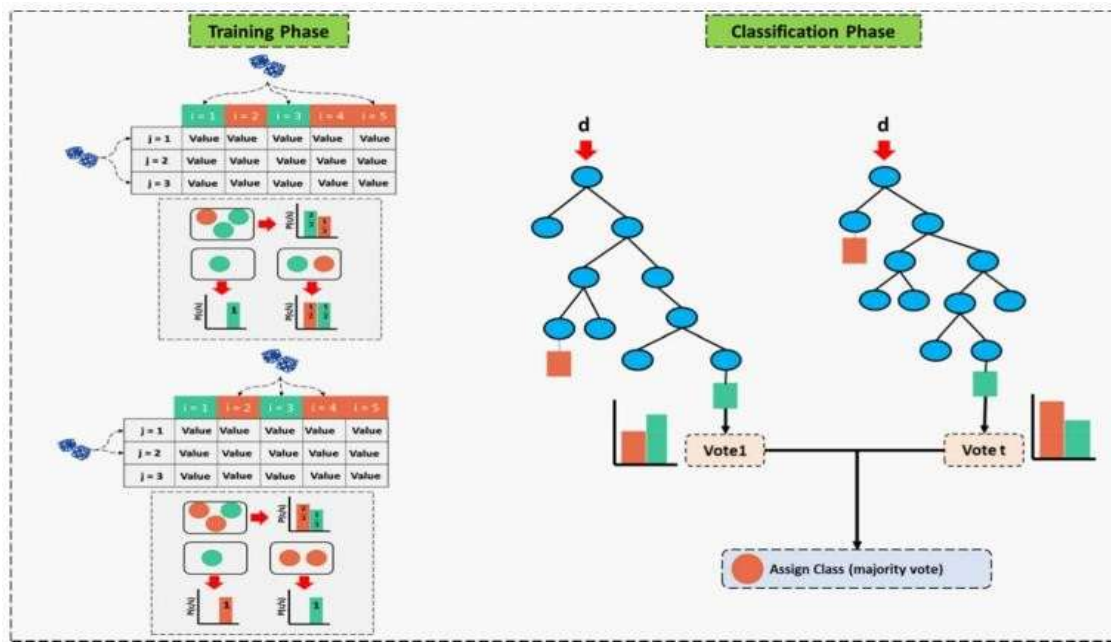


Figure 3.13: Training and classification phase of Random Forest classifier



Figure 3.14: Classification of training points

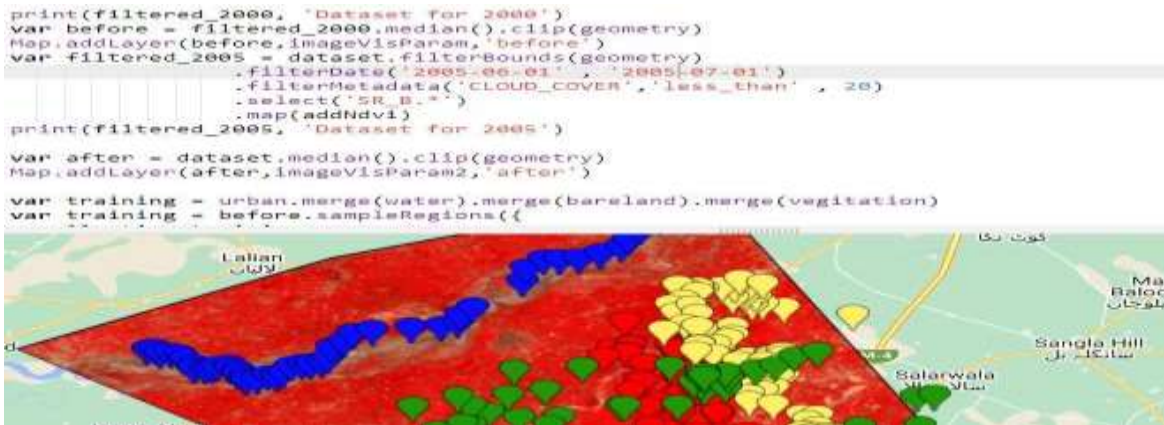


Figure 3.15: Image classification and merging samples for year 2000 and 2010

### 3.3.1 Random Forest (RF)

An ensemble learning method that constructs multiple decision trees during training. It operates by:  
Using decision trees as building blocks.

Employing random feature selection at each node to ensure diversity and reduce overfitting. Training on a labeled dataset with class-specific spectral information. The final classification is determined by a majority vote from all trees in the forest.

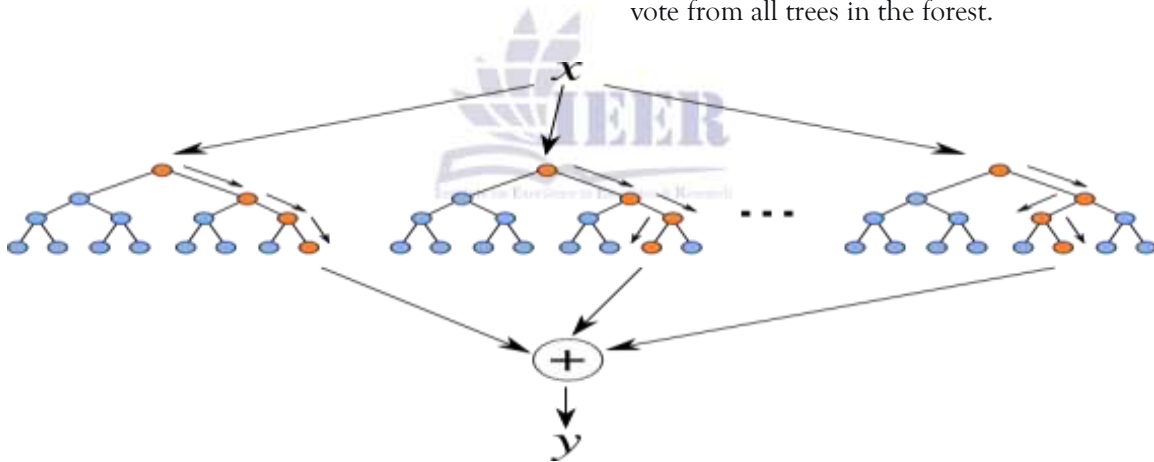


Figure 3.16: Random Forest classifier Technique

### 3.3.3 Classification and Regression Tree (CART)

A decision tree algorithm that recursively partitions the dataset based on feature values to create a model for prediction. It is interpretable and handles both categorical and numerical data but can be prone to overfitting without pruning. In this study, CART was

used to classify satellite images based on spectral features and indices.

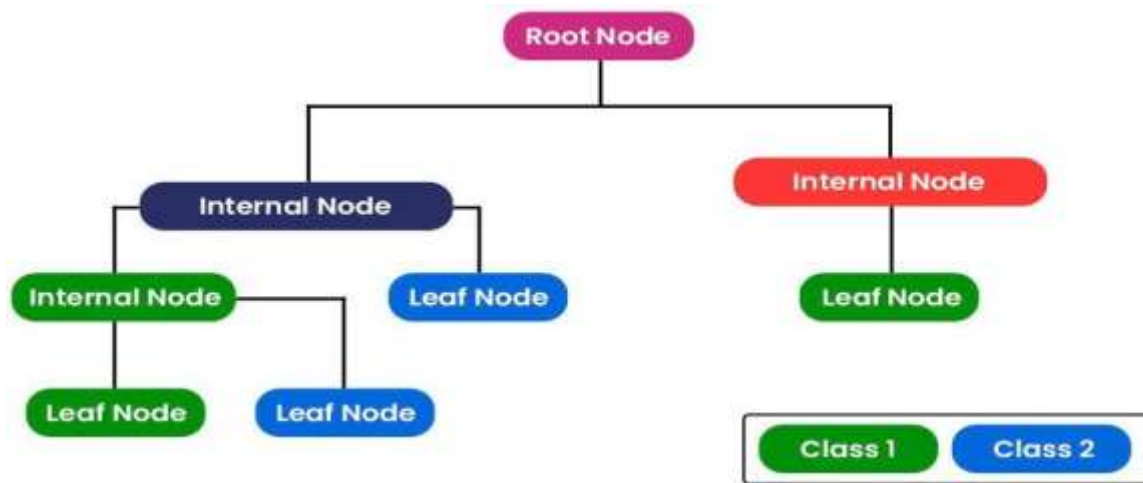


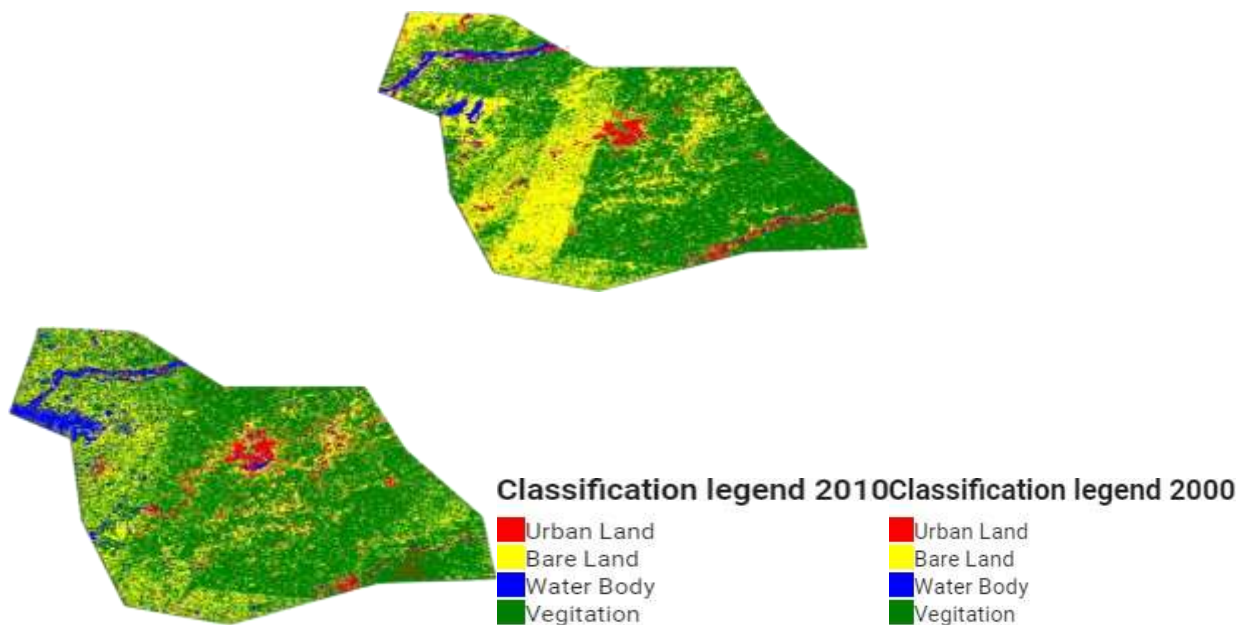
Figure 3.17: Typical decision tree for image classification

4: RESULTS AND DISCUSSION

This section presents the findings from the application of machine learning classifiers for Land Use Cover Change (LUCC) detection in Faisalabad Division (2000-2020), followed by an analysis of the results and their implications.

4.1 Machine Learning Classifiers

The study evaluated three classifiers: Support Vector Machine (SVM), Random Forest (RF), and Classification and Regression Tree (CART). The analysis revealed that the near-infrared band and NDVI were critical features for distinguishing land cover classes and detecting changes across different years. The models successfully generated annual land cover maps, with SVM demonstrating superior handling of mixed pixels and providing robust theoretical performance.



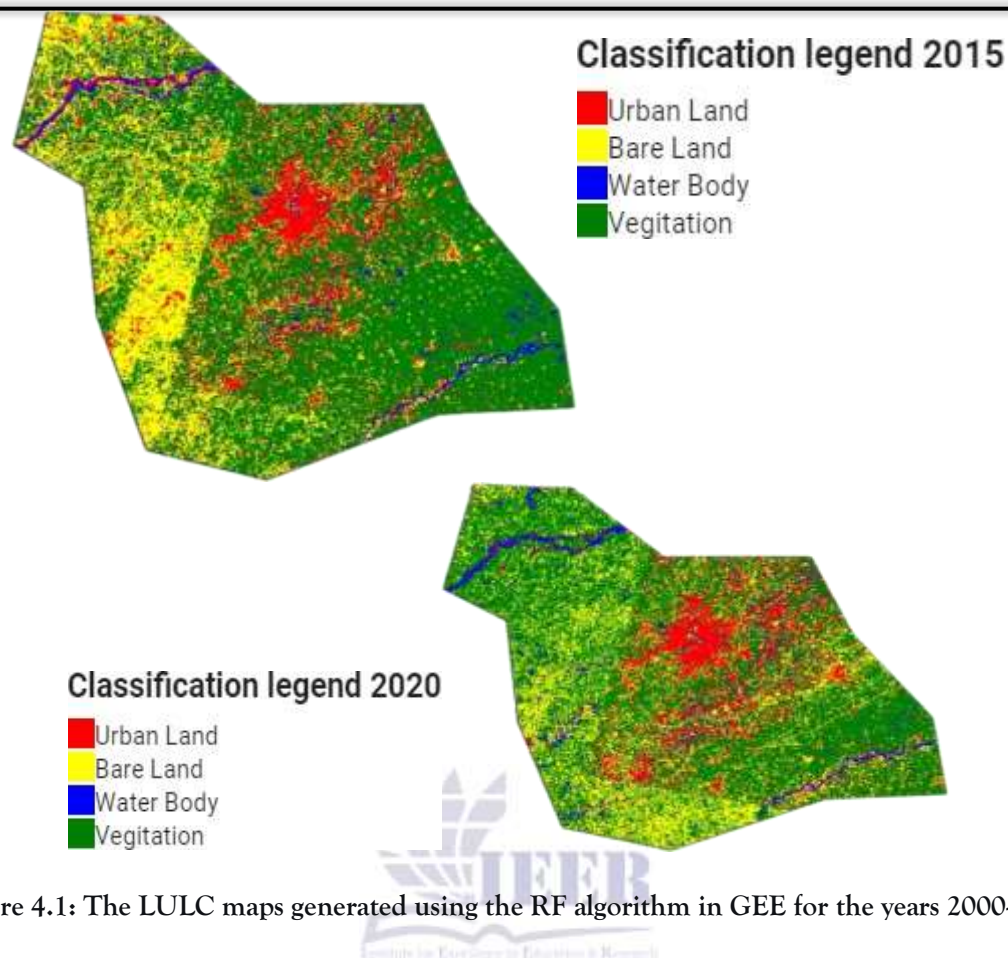


Figure 4.1: The LULC maps generated using the RF algorithm in GEE for the years 2000-2020

#### 4.2 Spatial Uncertainty of LUCC Maps

The land cover change analysis from 2000 to 2020 revealed a significant and continuous expansion of built-up areas in Faisalabad. This urban growth occurred primarily through the conversion of agricultural fields and natural vegetation into residential, commercial, and industrial zones. The spatial analysis quantified this transformation,

showing a substantial net increase in urban land cover over the two-decade period, accompanied by a corresponding decrease in green spaces and agricultural land.

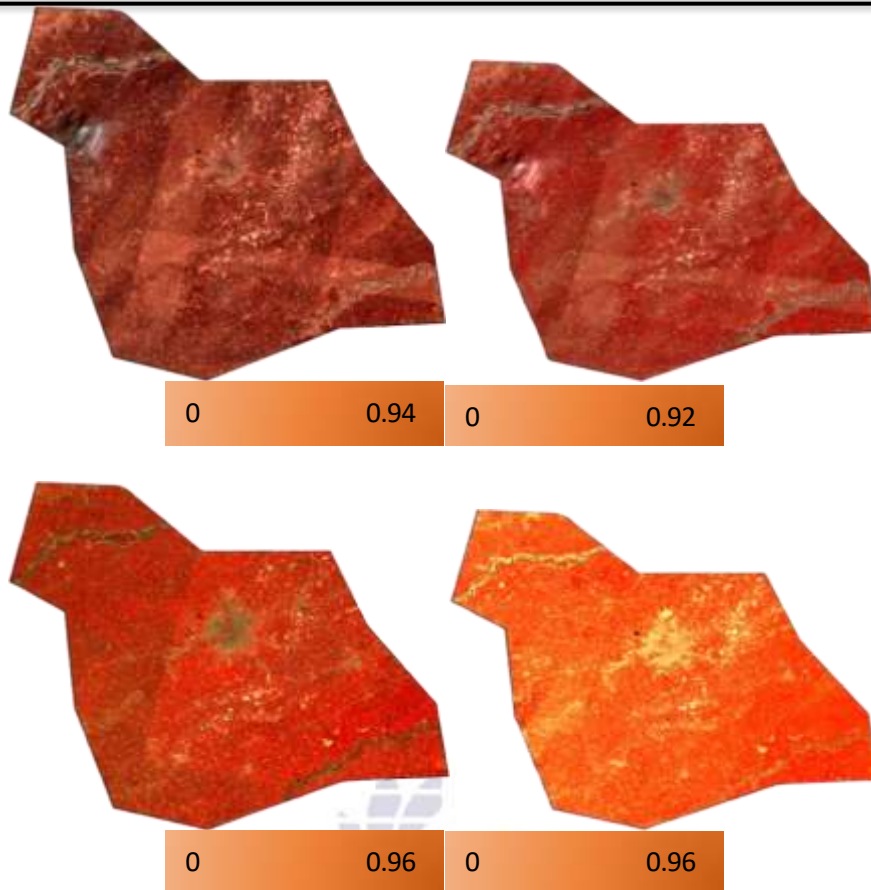


Figure 4.2: LUCC analysis for each year

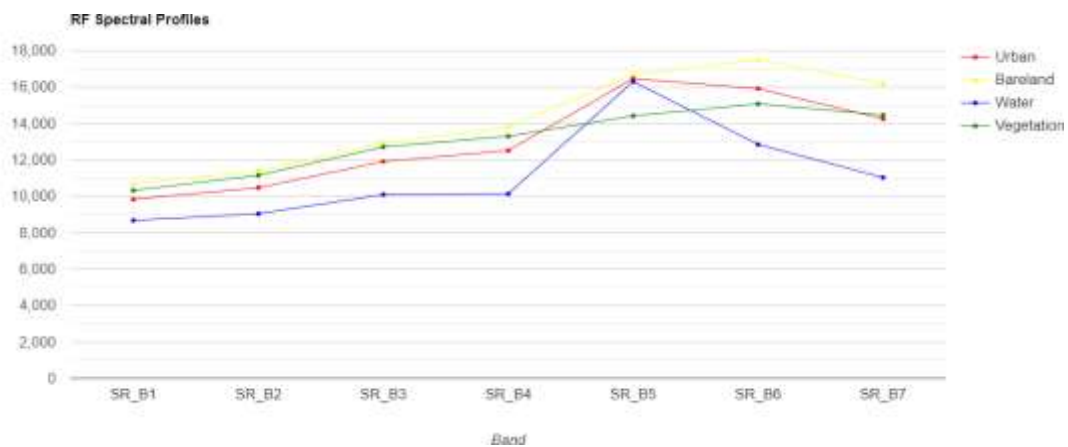


Figure 4.3: Changed Area of the maps for LUCC

### 4.3 Accuracy and Kappa Coefficient

A comprehensive accuracy assessment was conducted. The final LUCC maps produced by the SVM classifier were validated against reference data

from Google Earth Engine. The evaluation metrics Overall Accuracy and Kappa Coefficient confirmed the high performance of the multi-date composite

change detection approach in accurately identifying urban settlements and their changes over time.

	Parameter	2000	2010	2015	2020
SVM	Kappa Coefficient	88.59	89.66	96.33	97.37
	Overall accuracy	93.25	91.92	95.14	98.03
RF	Kappa Coefficient	83.34	88.9	86.37	96.8
	Overall accuracy	81.8	87.0	75.19	96.7
CART	Kappa Coefficient	70.2	60.45	68.0	74.3
	Overall accuracy	62.63	63.31	70.2	73.63

Table 4.1: Validation results for the machine learning algorithms

Classification algorithm	2000	2010	2015	2020
SVM	0.93	0.95	0.97	0.98
RF	0.92	0.94	0.96	0.96
CART	0.83	0.85	0.88	0.89

Table 4.2: Results of DST for spatial uncertainty analysis of the ULLC map

#### 4.4 Research Analysis

The primary objective was to assess the effectiveness of data-driven techniques within GEE for environmental monitoring. Among the three evaluated machine learning algorithms: SVM performed the best, achieving consistently high accuracies ranging from 90.25% to 98.03% across the study years. Its strength lies in managing mixed pixels and missing data. RF showed strong potential, with decent performance and resistance to noise due to its ensemble structure, though it yielded slightly lower accuracies than SVM. CART, while simple and interpretable, achieved the lowest accuracies. Its

decision-tree-based approach was less efficient for the complex spectral patterns inherent in LULC mapping for this study area.

#### 4.5 Discussion

##### 4.5.1 Overview of the Field

The field of land cover change detection in urban areas is crucial for environmental management and sustainable development. Remote sensing technologies, combined with data mining techniques, provide effective means to monitor temporal changes, offering vital insights for informed urban planning and policy-making.

#### 4.5.2 Gap Covered in the Research

This research addressed a specific gap by implementing a methodology originally proposed for general urban monitoring—to the specific context of Faisalabad, Pakistan. It localized the analysis, providing context-specific results on LUCC dynamics in a rapidly developing industrial and agricultural region.

#### 4.5.3 Research Contribution

The study made several key contributions:

**Data Acquisition & Preprocessing:** Acquired and preprocessed a dense time-series of Landsat data for Faisalabad.

**Land Cover Classification:** Applied the RF algorithm (alongside SVM and CART) to classify land cover into built-up areas, vegetation, and water bodies, utilizing NDVI for vegetation quantification.

**Change Detection & Analysis:** Identified and analyzed significant changes in urban/built-up areas over time, revealing trends and patterns of land use dynamics.

**Performance Evaluation:** Validated the classification results using ground truth data, ensuring the reliability and robustness of the methodological approach and findings.

### 5: SUMMARY AND CONCLUSIONS

This study successfully implemented a machine learning and remote sensing framework to detect and analyze urban land use/cover change (LUCC) in Faisalabad, Pakistan, from 2000–2020.

#### 5.1 Summary:

Using Google Earth Engine (GEE) and multi-temporal Landsat imagery, three classifiers SVM, RF, and CART were applied to monitor LUCC dynamics. NDVI and spectral bands were used as key features. SVM performed best (98.03% accuracy), followed by RF (96.7%) and CART (73.63%).

#### 5.2 Key Findings:

Built-up areas increased by over 60% by 2020.

Agricultural land, vegetation, and water bodies decreased by 40–80%.

Urban expansion occurred primarily at the expense of cropland and green cover.

#### 5.3 Recommendations:

To mitigate unchecked urban sprawl, we recommend

Establishing **urban growth boundaries**

Launching **agricultural land preservation programs**.

Promoting **urban agriculture** and **green belt zones**.

Implementing **smart land-use planning**.

#### 5.4 Conclusion:

The integration of GEE, Landsat data, and machine learning provides a powerful, replicable tool for monitoring urbanization. The results highlight urgent needs for sustainable land management in rapidly developing regions.

#### 5.5 Future Work:

Extend the study period for long-term trend analysis. Use higher-resolution imagery for detailed change detection.

Integrate climate data to assess environmental impacts on LUCC.

Apply the framework to other developing cities for comparative analysis.

### REFERENCES

- Adam, E., N.E. Masupha and S. Xulu. 2023. Spatial Assessment and Prediction of Urbanization in Maseru Using Earth Observation Data. *Appl. Sci.* 13:23-67.
- Angel, S., & Blei, A. M. (2018). Densify and expand: A global analysis of recent urban growth. *Sustainability*.10:2090.
- Antwi, E., Krawczynski, R., Wiegler, G., 2008. Detecting the effect of disturbance on habitat diversity and land cover change in a post-mining area using GIS. *Landsc. Urban Plan.* 87 :22–32.
- Atef, I., W. Ahmed and R.H. Abdel-Maguid. 2023. Modelling of land use land cover changes using machine learning and GIS techniques: a case study in El-Fayoum Governorate, Egypt. *Environ. Monit. Assess.* 195:456-487.
- Bai, T., L. Wang, D. Yin, K. Sun, Y. Chen, W. Li and D. Li. 2022. Deep learning for change detection in remote sensing: a review. *Geo-Spatial Inf. Sci.* 09:1–27.

- Basheer, S., X. Wang, A.A. Farooque, R.A. Nawaz, K. Liu, T. Adekanmbi and S. Liu. 2022. Comparison of Land Use Land Cover Classifiers Using Different Satellite Imagery and Machine Learning Techniques. *Remote Sens.* 14:1-18.
- Basommi, P., Guan, Q., Cheng, D., 2015. Exploring land use and land cover change in the mining areas of Wa East District, Ghana using Satellite Imagery. *Open Geosci.* 7:672-707.
- Breiman, L. (2001). Random forests. *Machine Learning*, 45, 5-32. Burges, C. J. C. (1998). A tutorial on support vector machines for pattern recognition. *Data Mining and Knowledge Discovery.* 2: 121-167.
- Çağlıyan, A. and D. Dağlı. 2022. Monitoring Land Use Land Cover Changes and Modelling of Urban Growth Using a Future Land Use Simulation Model (FLUS) in Diyarbakır, Turkey. *Sustain.* 14:87-103.
- Elmahdy, S.I. and M.M. Mohamed. 2023. Regional mapping and monitoring land use/land cover changes: a modified approach using an ensemble machine learning and multitemporal Landsat data. *Geocarto Int.* 38:457.
- Engine, G.E. 2022. Mapping of Land Cover with Optical Images, Supervised Algorithms, and Google Earth Engine. *sensors.* 34:1-19.
- Feizizadeh, B., D. Omarzadeh, M. Kazemi Garajeh, T. Lakes and T. Blaschke. 2023. Machine learning data-driven approaches for land use/cover mapping and trend analysis using Google Earth Engine. *J. Environ. Plan. Manag.* 66:665-697.
- Foody, G. M., & Mathur, A. (2004). Toward intelligent training of supervised image classifications: Directing training data acquisition for SVM classification. *Remote Sensing of Environment.* 93: 107-117.
- Friedl, M. A., & Brodley, C. E. (1997). Decision tree classification of land cover from remotely sensed data. *Remote Sensing of Environment.* 61.399-409.
- Friedl, M. A., McIver, D. K., Hodges, J., Zhang, X., Muchoney, D., Strahler, A., Woodcock, C. E., Gopal, S., Schneider, A., Cooper, A., Baccini, A., Gao, F., & Schaaf, C. (2002). Global land cover mapping from MODIS: Algorithms and early results. *Remote Sensing of Environment.* 83 : 287-302.
- Friedl, M. A., Sulla-Menashe, D., Tan, B., Schneider, A., Ramankutty, N., Sibley, A., & Huang, X. (2010). MODIS Collection 5 global land cover: Algorithm refinements and characterization of new datasets. *Remote Sensing of Environment.* 114:168- 182.
- Friedman, S. Z., & Angelici, G. (1979). The detection of urban expansion from Landsat imagery. *Remote Sensing Quarterly.*
- Real-time Bubble Sheet Detection and Evaluation Using Object Recognition. (2025). *The Asian Bulletin of Big Data Management* , 5(4), 32-42. <https://doi.org/10.62019/aqhpqx47>
- Seed Quality Detection Using Deep Learning Though RGB Camera. (2025). *The Asian Bulletin of Big Data Management* , 5(4), 43-59. <https://doi.org/10.62019/0t1qfy54>
- Zartasha Kiran, Awais Rasool, Kainat Shahid, & Nimra Razzaq. (2025). DETECTION OF IOT-BASED CYBER ATTACKS USING MACHINE LEARNING TECHNIQUES. *Spectrum of Engineering Sciences*, 3(10), 884-898. Retrieved from <https://www.thesesjournal.com/index.php/1/article/view/1270>
- Candido, C., A.C. Blanco, J. Medina, E. Gubatanga, A. Santos, R.S. Ana and R.B. Reyes. 2021. Improving the consistency of multi-temporal land cover mapping of Laguna lake watershed using light gradient boosting machine (LightGBM) approach, change detection analysis, and Markov chain. *Remote Sens. Appl. Soc. Environ.* 23:100565.
- Candido, C., A.C. Blanco, J. Medina, E. Gubatanga, A. Santos, R.S. Ana and R.B.

- Chellasamy, M., T.P.A. Ferré, M.H. Greeve, R. Larsen and U. Chinnasamy. 2014. An ensemble classification approach for improved land use/cover change detection. *Int. Arch. Photogramm. Remote Sens. Spat. Inf. Sci.*8:695-701.
- Deng, Z. 2023. Intensity Analysis to Communicate Detailed Detection of Land Use and Land Cover Change in Chang-Zhu-Tan Metropolitan. *Remote Sens.* 34:674-746.
- Din, S.U. and H.W.L. Mak. 2021. Retrieval of land-use/land cover change (Lucc) maps and urban expansion dynamics of hyderabad, pakistan via landsat datasets and support vector machine framework. *Remote Sens.* 13:1-25.

